A kinetic lattice-gas model for the triangular lattice with strong dynamic correlations. I. Self-diffusion

1994 J. Phys.: Condens. Matter 6 7633

(http://iopscience.iop.org/0953-8984/6/38/005)

J. Phys.: Condens. Matter 6 (1994) 7633–7653. Printed in the UK

A kinetic lattice-gas model for the triangular lattice with strong dynamic correlations: I. Self-diffusion

J Jäckle and A Krönig†
Fakultät für Physik, Universität Konstanz, Postfach 5560 M679, D-78434 Konstanz, Germany

Received 5 April 1994, in final form 5 July 1994

Abstract. Self-diffusion in a lattice-gas model with two-vacancy assisted hopping on the triangular lattice is investigated, by both Monte Carlo simulation and analytical calculation. A very rapid decrease of the tracer-correlation factor and marked size effects in finite lattices give evidence for strong dynamic correlations in both space and time at high particle concentration. Although the decrease of the self-diffusion coefficient over 3.5 decades for concentrations up to $c = 0.77$ is best fitted by a power law $(0.835 - c)^{3.54}$, it is argued that the model does not have a sharp dynamical phase transition with a critical concentration lower than one. The argument is based on a proof of absence of permanently blocked particles in infinite lattices at all concentrations below one. The self-diffusion coefficient is calculated analytically within a pair approximation which gives good results for lower concentrations, but fails at the higher concentrations. The approximation is in qualitative agreement with the Monte Carlo data for the tracer-correlation factor at all concentrations for a variant of the model with one-vacancy assisted hopping, in which the dynamic correlations are less pronounced.

1. Introduction

It is commonly accepted that the non-vibrational motions of molecules in supercooled liquids develop strong dynamic correlations in space and time, before this type of motion is arrested at the glass transition. Diffusion models with the simplified geometry of a lattice are attractive for studying such correlations and their observable consequences. In the past several models of this kind have been investigated: the hard-rod lattice gas [1], the hard-square lattice gas [2–8], and, most recently, the lattice gas with four-vacancy assisted hopping on the simple cubic lattice [9]. The model presented here has the advantage of relative simplicity, which makes it suitable for a test of several established approximation schemes of analytical theory. The pair approximation, which is successful for simple lattice gases without further kinetic constraint [10, 11], is applied to the calculation of the self-diffusion coefficient. Application of a mode-coupling approximation is deferred to paper II [17], which deals with properties of collective diffusion rather than self-diffusion.

This paper is organized as follows. After the model is introduced in section 2, Monte Carlo results for quantities characterizing self-diffusion, such as the mean square displacement, incoherent intermediate scattering function, self-diffusion coefficient and tracer-correlation factor, are presented in section 3. In section 4 it is shown that permanently blocked particles do not exist in the thermodynamic limit of infinite lattice size. Section 5 contains the analytical calculation of the self-diffusion coefficient. A two-dimensional and

† Present address: Institut für Grundlagen der Elektrotechnik, Technische Universität Dresden, D-01069 Dresden, Germany.

0953-8984/94/387633+21$19.50

a three-dimensional variant of the model are treated in section 6. Section 7 is concerned with size effects in diffusion and the characteristic length related to these, and a summary is given in section 8.

2. The model

The model is a lattice gas on the two-dimensional triangular lattice with two-vacancy assisted diffusion dynamics. A lattice site can be occupied only by one particle at a time. There is no interaction potential between different particles. In equilibrium at concentration c every lattice site is occupied by a particle with probability c, independent of the occupation of other sites. Therefore there are no static correlations. A particle can jump to an empty nearest-neighbour site only under the condition that the two sites on either side of the jump path are vacant (figure 1). This is the kinetic constraint in the model. For a jump from site i to $i+\delta$, where δ is one of the six nearest-neighbour vectors, we denote these two sites by $i+o(\delta)$ and $i+u(\delta)$ (see section 4). The attempt frequency Γ for the jump of a particle to a nearest-neighbour site is set equal to one. Jumps to more distant sites are not considered.

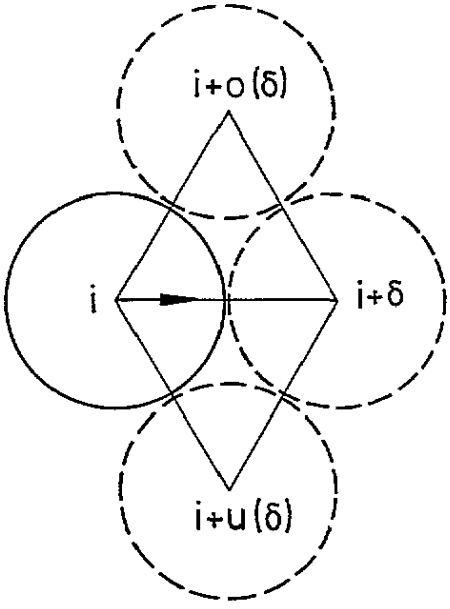

Figure 1. The kinetic constraint for a particle on the triangular lattice to jump from site i to a nearest-neighbour site $i+\delta$. The circles (full line for the particle and dashed lines for the vacancies) illustrate the geometric interpretation of the constraint (see text).

This model is designed as a model for cooperative dynamics rather than for a concrete physical system, like hydrogen in metals [12, 13]. The kind of cooperativity we have in mind is thought to occur in the slow diffusive molecular motion in supercooled liquids near the glass transition [14]. A characteristic feature of such cooperativity is that neither a single vacancy nor any complex of vacancies can propagate through a full lattice without the assistance of additional vacancies. If particles are arranged in a straight line, with no

vacant sites in between, they block each other mutually. In lattices of finite size, such lines may form 'cages' of permanently blocked particles (section 6). As shown below (section 2), the diffusion process slows down extremely quickly at higher particle concentrations, which is in qualitative accord with the behaviour of supercooled liquids. The model shares the properties of cooperativity with the hard-square lattice gas [4, 5, 7], but is simpler to handle, both by computer simulation and analytically, due to its lack of static correlations.

Although the model is not claimed to represent a concrete physical system, it is of interest to note that its kinetic constraint has a geometric interpretation. On a triangular lattice with lattice constant a all sites may be occupied randomly by hard-disc particles with a diameter $d \leqslant a$. However, if it is assumed that the centres of the particles can move only along the edges of the triangular lattice, the jump of a particle to an empty nearest-neighbour site is subject to a condition if the disc diameter d is larger than the critical value of $(\sqrt{3}/2)a$. The condition is that both sites adjacent to the jump path are vacant, which is the kinetic constraint of our model.

Several variants of the model are described in section 5.

3. Results of Monte Carlo simulation

We first present the results of Monte Carlo simulation for two quantities characterizing self-diffusion: the mean square displacement $\langle(\Delta r)^2\rangle_t$ and the incoherent intermediate scattering function $F_s(k, t)$. The latter is the characteristic function of the displacement $\Delta r(t)$ of a particle during a time interval of length t, and is defined by

$$F_s(k, t) = \langle \exp(ik \cdot \Delta r)\rangle_t. \tag{1}$$

Figure 2 is a log–log plot of the ratio $\langle(\Delta r)^2\rangle_t/t$ against time for different concentrations. The long-time limit of this ratio determines the self-diffusion coefficient D_s, namely

$$\lim_{t\to\infty} \langle(\Delta r)^2\rangle_t/t = 4D_s. \tag{2}$$

For arbitrary times, the ratio may be interpreted analogously in terms of a time-dependent coefficient of self-diffusion $D_s(t)$. While at low concentrations the difference between the short-time and the long-time diffusion coefficient is small, and the transition between them occurs in a relatively short time region, at higher concentrations this difference becomes very large, and the transition region extends to very long times. At $c = 0.8$ (lowest curve in figure 2) the long-time limit is not reached within the length of our MC runs of 10^6 MC steps per particle. This qualitative behaviour of the curves shown in figure 2 can be ascribed [15] to an increasing degree of backward correlation of jump directions with increasing particle density. The ratio between the short-time and the long-time limit of $D_s(t)$, which defines the tracer-correlation factor f_s, is considered below (section 5).

Figure 3 shows two different fits of our Monte Carlo data for the concentration-dependent self-diffusion coefficient $D_s(c)$. Surprisingly, the data can be fitted almost equally well by two very different formulae: the power-law formula

$$D_s(c) = A(0.835 - c)^\nu \tag{3}$$

with coefficient $A = 2.26$ and exponent $\nu = 3.54$, and the exponential formula

$$D_s = B \exp[-a/(1 - c)] \tag{4}$$

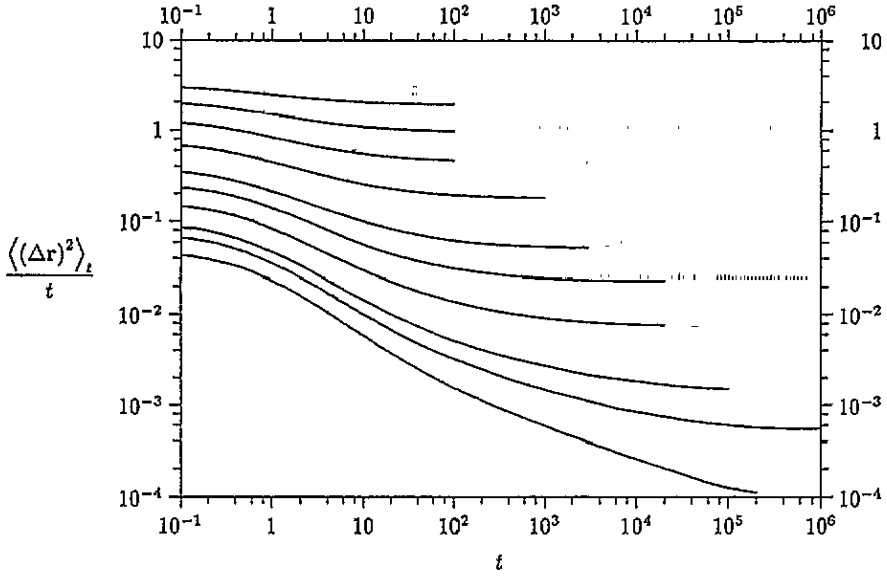

Figure 2. Mean square displacement divided by the time for particle concentrations $c = 0.2$, 0.3, 0.4, 0.5, 0.6, 0.65, 0.7, 0.75, 0.77 and 0.8 (from the top).

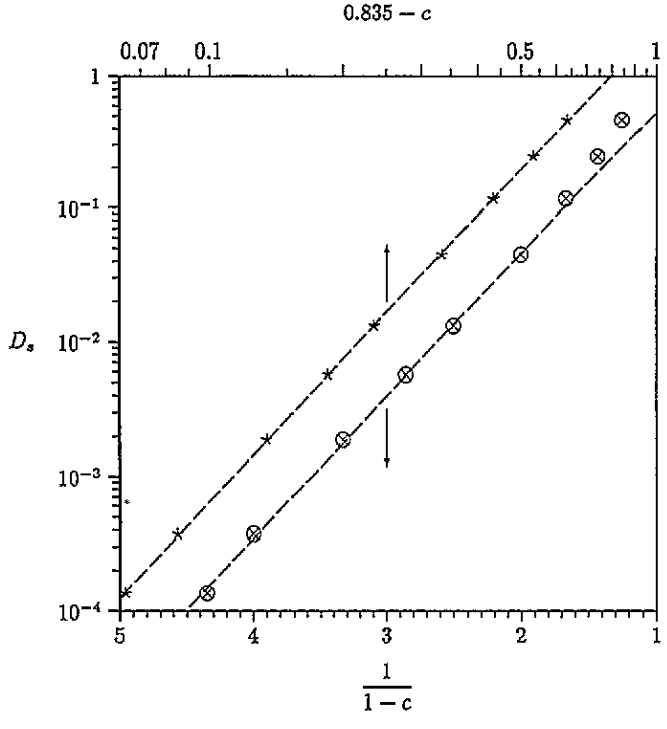

Figure 3. Two different plots of the self-diffusion coefficient as a function of particle concentration. The straight lines are the fits equations (3) and (4).

with coefficients $B = 6.05$ and $a = 2.44$. The first fit, which is slightly better than the second one, extrapolates to a vanishing self-diffusion coefficient at a critical concentration $c^* = 0.835$. On the other hand, extrapolation using the second formula predicts the self-diffusion coefficient to vanish only at $c = 1$, though with an essential singularity. In the following we argue that the self-diffusion coefficient for an infinite lattice should be positive at any concentration $c < 1$. Accordingly, for an extrapolation of $D_s(c)$ outside the range of the Monte Carlo data the second fit is to be preferred. We do not expect, however, that the fit (4) is the asymptotic concentration dependence of $D_s(c)$ for $c \to 1$. Experience from the calculation of the characteristic length (subsection 7.2) leads us to expect that the asymptotic formula may only hold at concentrations far beyond the range of our Monte Carlo data for the self-diffusion coefficient.

Regarding the surprising indifference of our $D_s(c)$ data to fits by two very different expressions, we note that even close to the singularity at $x = 0$ the function $y = \exp(-1/x)$ can be approximated well by power laws $(x - x_0)^\nu$ in limited x intervals. This is due to the fact that $y(x)$ for $x > x_0$ and any $x_0 > 0$, if plotted against $(x - x_0)$ in doubly logarithmic form, yields a curve with an inflection point at $x = 2x_0$, near which it is well approximated by a straight line. One can show, e.g., that for the interval $1.25x_0 \leqslant x \leqslant 5x_0$ a power law $(x - x_0)^\nu$ with exponent $\nu = 0.229/x_0$ approximates $y(x)$ in a log–log plot to within 2.5% of its total variation in this plot, which amounts to $\alpha = 0.276/x_0$ decades. Therefore, close to the singularity at $x = 0$, the variation of $y(x)$ over several decades within an x interval spanning a factor of four can be well approximated by a power law proportional to $(x - x_0)^\nu$ on a doubly logarithmic plot. This relation between the seemingly different functions (3) and (4) explains why it is possible for our $D_s(c)$ data to be fitted by either of them.

We point out that this ambiguity of fitting is not a peculiarity of the self-diffusion coefficient of our model. A parallel can be drawn to the observed temperature dependence of the shear viscosity of real fluids. According to [16], for a wide variety of fluids in the low-viscosity regime, both above and below the melting point, a power law fits the increase of the shear viscosity with decreasing temperature equally well as or better than the Arrhenius or Vogel–Fulcher formulae. The Arrhenius and Vogel–Fulcher formulae are to be compared with our exponential formula (4), from which they can be obtained if a linear temperature dependence of the concentration due to thermal expansion is assumed for the lattice gas. The viscosity data were found to follow a power law over one or two decades only, whereas our data cover $3\frac{1}{2}$ decades of the self-diffusion coefficient. However, compared with a total increase of the viscosity towards the glass transition by about thirteen decades, even this corresponds only to incipient freezing. We conclude that the situation concerning the concentration dependence of the self-diffusion coefficient of our model is analogous to that encountered for the incipient increase with decreasing temperature of the shear viscosity of real fluids.

Finally, some of our Monte Carlo results for the incoherent intermediate scattering function $F_s(k, t)$ are presented. Figure 4 shows a time-scaled semi-logarithmic plot of $F_s(k, t)$ for different concentrations c for one particular wavevector k, which corresponds to $\kappa = (\pi, 0)$. (For the relation between k and κ see section 5, equation (18).) The scaling time $\tau(c)$ is determined by the decay of the scattering function from 1 to 1/e. According to figure 5, it increases very rapidly with increasing particle density. The time dependence of $F_s(k, t)$ is nearly exponential at the lowest concentrations shown. For higher concentrations it becomes more and more stretched exponential. A limiting scaled form of the time dependence at high concentrations is not found in the c range investigated. Neither is there an indication of a two-stage behaviour in the decay of the scattering function. We

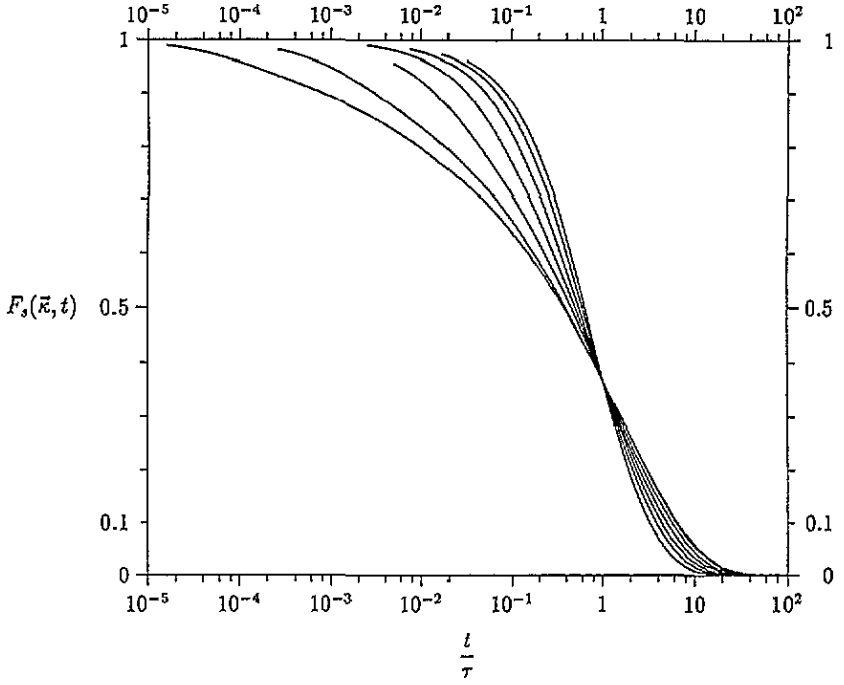

Figure 4. Incoherent intermediate scattering function $F_s(k,t)$ for $\kappa = (\pi, 0)$ against scaled time t/τ at concentrations $c = 0.2, 0.3, 0.4, 0.5, 0.6, 0.7$ and 0.75 (from right to left in the upper part of the figure).

anticipate, however, that for the *coherent* intermediate scattering function of our model two-stage decay is observed at high concentration and for large wavevector [17].

4. Absence of permanently blocked particles in the thermodynamic limit

Our argument for a non-zero coefficient of self-diffusion at all concentrations lower than one is based on the absence of permanently blocked particles in the thermodynamic limit. By this we mean that, if the lattice is sufficiently large, there is always a way of making an initially blocked particle able to jump. With increasing particle concentration the required process of letting other particles jump first becomes longer and longer and more and more cumbersome. The fact that it is kinetically always possible to make any particle jump, of course, does not *prove* that normal diffusion with non-zero self-diffusion coefficient persists at all concentrations lower than one. It would be possible that above a certain critical concentration smaller than one self-diffusion is anomalous in the sense that the long-time limit (2) is zero. However, we think it is most likely that the trend of the concentration dependence of self-diffusion shown in figure 2 continues to higher concentrations without any qualitative change: we expect the intermediate-time region, in which the mean square displacement grows sublinearly, to become more and more extended, so that at very high concentrations self-diffusion practically *is* anomalous, although the mathematical infinite-time limit (2) still is not zero. A similar situation is met for the hard-square lattice gas and, with relaxation by single-spin flips, for the two-spin facilitated kinetic Ising model [18, 19].

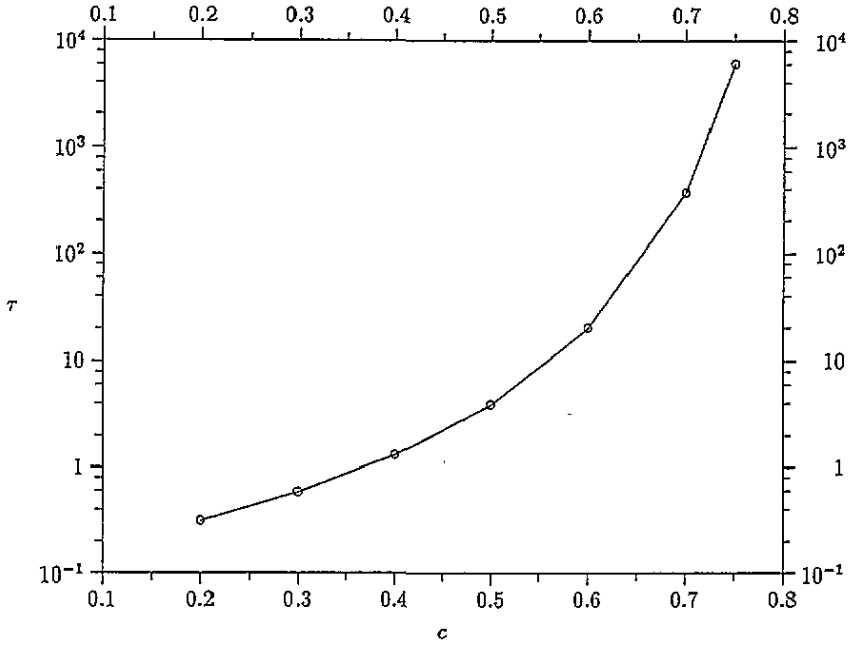

Figure 5. The average relaxation time τ derived from the incoherent intermediate scattering function $F_s(k, t)$ for $\kappa = (\pi, 0)$ as a function of particle concentration c.

Our expectation is also supported by the results for the characteristic length (subsection 7.2), which extend to higher concentrations.

The absence of permanently blocked particles in the thermodynamic limit follows from a proof that a hexagonal ring of vacancies can grow to infinite size. In the course of this process every particle on the lattice jumps at the moment it is passed by the growing ring. The idea underlying the proof is similar to that of the 'large-void instability' known in certain bootstrap-percolation models [20]. The proof, which is similar to that given for the hard-square lattice gas, is only sketched here.

The growth of a hexagonal ring of vacancies is illustrated in figure 6. Here the ring of the fourth-nearest neighbours of a central site is completely empty. (The occupation of the lattice inside this ring is irrelevant.) Let us denote the size of this ring by the length of any of its six edges, which is $l = 4$. If there is at least one vacancy per edge on the adjacent ring of size $l = 5$, all particles on this outer ring can jump onto the inner ring, so that the ring of vacancies grows in size by one. This leads to the following recursion relation for the probability p_l that the ring of vacancies grows to size l:

$$p_l = p_{l-1}\left[1 - c^l\right]^6. \tag{5}$$

(Strictly speaking, this is a lower bound.) Putting $p_0 = 1$, relation (5) holds for all $l \geqslant 1$. It is not difficult to show that the solution of this recursion relation for $l \to \infty$ converges to a non-zero limit p_∞, which can be estimated for $c = 1 - \epsilon \to 1$ approximating $\ln(1 - c^l)$ by $\ln(l\epsilon)$ for $1 \leqslant l \leqslant \epsilon^{-1}$ and by $(-\exp(-l\epsilon))$ for $l > \epsilon^{-1}$ and replacing the sum over l for p_∞ by an integral. The approximate result obtained reads

$$p_\infty \simeq \exp\left(-\frac{6(1 + e^{-1})}{\epsilon}\right). \tag{6}$$

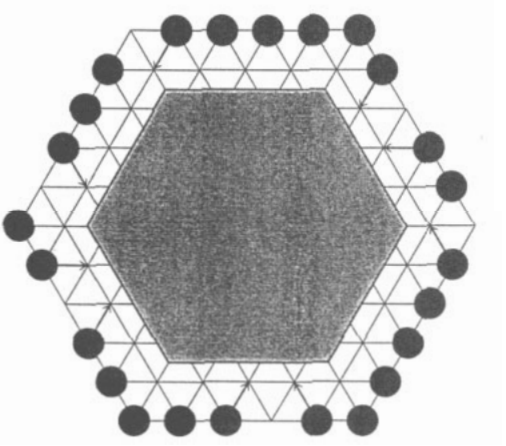

Figure 6. Growth of a hexagonal ring of vacancies. The arrows indicate the first of a sequence of particle jumps by which the outer ring is vacated.

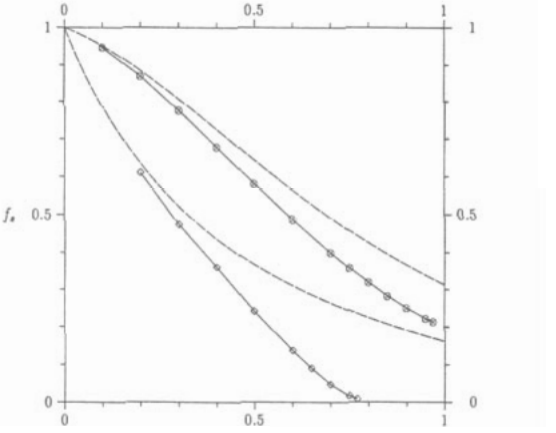

Figure 7. Comparison of Monte Carlo data (full line) with the result of an analytical calculation (dashed line) for the tracer-correlation factor. The pair of upper curves is obtained for the modified model with one-vacancy assisted hopping (subsection 6.1).

Solving (5) numerically, one finds the asymptotic formula for $\epsilon \to 0$

$$p_\infty \sim \exp(-9.870/\epsilon) \tag{7}$$

which has the same functional form as (6), but the coefficient in the exponent is 20% larger. The convergence of p_l to a non-zero limit p_∞ implies that the growth process continues to infinity almost with certainty once the ring of vacancies has reached a certain critical size of order ϵ^{-1}. Since in an infinite lattice there are infinitely many independent attempts of growth to this critical size, at least one of them is successful with certainty. A rigorous formulation of this second part of the proof requires some care and is not undertaken here. We refer to the analogous case for the hard-square lattice gas [7].

5. Calculation of the self-diffusion coefficient in a pair approximation

We calculate the self-diffusion coefficient D_s for our model in a pair approximation, which describes the motion of the tracer particle and a vacancy. If applied to self-diffusion in the simple lattice gas, where additional vacancies are not required for a particle to jump, this approximation yields the exact result for $D_s(c)$ asymptotically for $c \to 1$ [21] and is equivalent to the treatment of this problem by Tahir–Kheli and Elliott [10, 11].

5.1. Method of calculation

D_s is derived from the space- and time-dependent tracer correlation function $S_i(t)$, which is defined as

$$S_i(t) = \Omega\langle p_0(0)p_i(t)\rangle \tag{8}$$

where $p_i(t)$ is the occupation number for the occupation of site i by the tracer particle at time t, and Ω is the number of sites of the finite lattice. The brackets $\langle\ldots\rangle$ denote

the average over an equilibrium ensemble. At the same time, $S_i(t)$ is also the conditional probability that the tracer particle is at site i at some time $t > 0$ if it has been at the origin at time zero. The self-diffusion coefficient is obtained from the Fourier–Laplace transform of this function, defined by

$$\tilde{S}(\kappa, s) = \int_0^\infty \mathrm{d}t\, \mathrm{e}^{-st} \sum_i \mathrm{e}^{-\mathrm{i}\kappa n(i)} S_i(t) \tag{9}$$

as

$$D_s^{-1} = \lim_{\kappa \to 0} \lim_{s \to 0} k^2(\kappa) \tilde{S}(\kappa, s). \tag{10}$$

To explain the meaning of $n(i)$ and $k(\kappa)$ in the above expressions, we first need to recall some properties of the triangular lattice and its reciprocal lattice.

So far lattice vectors have simply been denoted by i. The position vector $r(i)$ of a site of the triangular lattice (which will have a lattice constant of one) is a linear combination of the basis vectors

$$a_1 = (1, 0) \qquad a_2 = \tfrac{1}{2}(1, \sqrt{3}) \tag{11}$$

with integers $n_1(i)$ and $n_2(i)$:

$$r(i) = \sum_{\alpha=1,2} n_\alpha(i) a_\alpha. \tag{12}$$

The last equation defines a mapping $r(n)$ of the square lattice (with lattice constant one) on the triangular lattice. The six shortest non-zero vectors of the triangular lattice, which mark the six nearest neighbours to the origin, are obtained as $r(\delta)$ for the six integer vectors

$$\begin{aligned} &\delta_1 = \quad (1, 0) \qquad \delta_2 = (0, 1) \qquad \delta_3 = (-1, 1) \\ &\delta_4 = (-1, 0) \qquad \delta_5 = (0, -1) \qquad \delta_6 = (1, -1). \end{aligned} \tag{13}$$

The inverse of equation (12), which maps the triangular lattice on the square lattice, reads

$$n(r) = \sum_{\alpha=1,2} x_\alpha b_\alpha / 2\pi \tag{14}$$

where $r = (x_1, x_2)$, and

$$b_1 = 2\pi \left(1, -\frac{1}{\sqrt{3}}\right) \qquad b_2 = 2\pi \left(0, \frac{2}{\sqrt{3}}\right) \tag{15}$$

are the basis vectors of the reciprocal lattice. Taking advantage of the mapping (12), spatial Fourier transform of functions on the triangular lattice can be conveniently performed on the square lattice:

$$\tilde{f}(\kappa) = \sum_n \mathrm{e}^{-\mathrm{i}\kappa n} f(n). \tag{16}$$

The inverse transformation reads

$$f(n) = \int\int \frac{\mathrm{d}\kappa_1 \mathrm{d}\kappa_2}{(2\pi)^2} \mathrm{e}^{-\mathrm{i}\kappa n} \tilde{f}(\kappa) \tag{17}$$

where the integration over κ_1 and κ_2 extends from $-\pi$ to $+\pi$. The wavevector k reciprocal to the position vector r on the triangular lattice is given in terms of κ by

$$k = \sum_{\alpha=1,2} \kappa_\alpha b_\alpha / 2\pi \tag{18}$$

from which the relation

$$k \cdot r = \kappa \cdot n \tag{19}$$

follows. The square of $k(\kappa)$, which occurs in formula (10), is obtained as

$$\big(k(\kappa)\big)^2 = \tfrac{4}{3}(\kappa_1^2 + \kappa_2^2 - \kappa_1\kappa_2). \tag{20}$$

To obtain a formal scheme of calculation, the tracer correlation function $S_i(t)$ is expressed as a scalar product of the two factors p_0 and $p_i(t)$. The general definition of the scalar product is as follows. A set of occupation numbers n_i for all lattice sites, for occupation by *any* particle, together with the site occupied by the tracer particle defines a state ω. For two functions A and B of this state the scalar product is defined as

$$(A, B) = \sum_{\omega} \rho_0(\omega)\big(A(\omega)\big)^* B(\omega) \tag{21}$$

where $\rho_0(\omega)$ is the equilibrium probability of state ω. (In the absence of a potential energy, $\rho_0(\omega)$ depends only on the total number of particles in the state.) With normalized tracer occupation numbers

$$A_i = \sqrt{\Omega} p_i \tag{22}$$

the tracer correlation function can now be written as

$$S_i(t) = \big(A_0, A_i(t)\big). \tag{23}$$

The time dependence of the factor $A_i(t)$ in this expression is generated by an operator L^+, which is the Hermitian adjoint of the Liouville operator defined by the Master equation for our model. The expression for $A_i(t)$ reads

$$A_i(t) = \exp(L^+ t) A_i. \tag{24}$$

The operator L^+ acts on any state function $A(\omega)$ as

$$L^+ A(\omega) = \frac{1}{2} \sum_{i,\delta} w_{i,\delta}(\omega) \left[A\left(\omega^{(i,\delta)}\right) - A(\omega) \right]. \tag{25}$$

The sum on the RHS (including the factor $\frac{1}{2}$) extends over all pairs of nearest-neighbour sites $(i, i+\delta)$. $\omega^{(i,\delta)}$ is the state obtained from ω by interchanging the occupation of these sites. The rate $w_{i,\delta}$ of this interchange (with an attempt frequency of one) is given by

$$w_{i,\delta}(\omega) = (1 - n_i n_{i+\delta})(1 - n_{i+o(\delta)})(1 - n_{i+u(\delta)}) \tag{26}$$

where for the six nearest-neighbour vectors δ_α ($\alpha = 1, \ldots, 6$) $o(\delta_\alpha)$ and $u(\delta_\alpha)$ are defined as

$$o(\delta_1) = \delta_2 \qquad u(\delta_2) = \delta_1 \qquad \text{and cyclic permutation.} \tag{27}$$

The first factor on the RHS of (26) forbids the simultaneous occupation of the two sites i and $i + \delta$, between which a particle jump occurs. (This factor cancels in the case of collective diffusion where no particle is marked.) The second and third factors express the condition that the two sites on either side of the jump path must be vacant.

We evaluate (23) within a subspace of state functions in which the motion of a tracer-particle–vacancy pair can be described. This subspace is spanned by the orthonormal set of functions A_i and B_i^Δ, where B_i^Δ is defined by

$$B_i^\Delta = A_i \frac{\Delta n_{i+\Delta}}{\sqrt{c(1-c)}} \qquad (\Delta \neq 0) \tag{28}$$

with $\Delta n = n - c$.

5.2. Equations of motion

From the matrix elements of L^+ for A_i and B_i^Δ one obtains the equations of motion for the coupled correlation functions $S_i(t)$ and $S_i^\Delta(t)$, the latter of which is defined as

$$S_i^\Delta(t) = (A_0, B_i^\Delta(t)). \tag{29}$$

The first of these equations reads

$$\begin{aligned}\frac{\mathrm{d}}{\mathrm{d}t}S_i(t) = &-(1-c)^3 \sum_\delta (S_i(t) - S_{i+\delta}(t)) \\ &+ \sqrt{c(1-c)}(1-c)^2 \sum_\delta \left(3S_i^\delta(t) - S_{i-\delta}^\delta(t) - S_{i-o(\delta)}^\delta(t) - S_{i-u(\delta)}^\delta(t)\right).\end{aligned} \tag{30}$$

The equation of motion for $S_i^\Delta(t)$ depends on whether Δ is one of the nearest-neighbour vectors δ or not. In the first case one has

$$\begin{aligned}\frac{\mathrm{d}}{\mathrm{d}t}S_i^\delta(t) = &\sqrt{c(1-c)}(1-c)^2\left(3S_i(t) - S_{i+\delta}(t) - S_{i+o(\delta)}(t) - S_{i+u(\delta)}(t)\right) + 6(1-c)^3 S_i^\delta(t) \\ &- (1-c)^2 \sum_{\delta'}\left(S_i^\delta(t) - S_i^{\delta+\delta'}(t)\right) - (1-c)^3 \sum_{\delta'}\left(S_i^\delta(t) - S_{i-\delta'}^{\delta+\delta'}(t)\right) \\ &+ (1-c)^2\left((2c-1)S_{i+u(\delta)}^{o(\delta)}(t) - (2c+1)S_i^{o(\delta)}(t)\right) \\ &+ (1-c)^2\left((2c-1)S_{i+o(\delta)}^{u(\delta)}(t) - (2c+1)S_i^{u(\delta)}(t)\right) \\ &+ c(1-c)^2\left(S_{i+u(\delta)}^{-u(\delta)}(t) + S_{i+\delta}^{-u(\delta)}(t) - S_i^{-u(\delta)}(t)\right) \\ &+ c(1-c)^2\left(S_{i+o(\delta)}^{-o(\delta)}(t) + S_{i+\delta}^{-o(\delta)}(t) - S_i^{-o(\delta)}(t)\right) \\ &+ c(1-c)^2\left(S_{i+\delta}^{-\delta}(t) + S_{i+u(\delta)}^{-\delta}(t) + S_{i+o(\delta)}^{-\delta}(t)\right).\end{aligned} \tag{31}$$

Otherwise, for $\Delta \neq \delta$, the simpler equation

$$\frac{\mathrm{d}}{\mathrm{d}t}S_i^\Delta(t) = -(1-c)^2 \sum_\delta \left(S_i^\Delta(t) - S_i^{\Delta+\delta}(t)\right) - (1-c)^3 \sum_\delta \left(S_i^\Delta(t) - S_{i-\delta}^{\Delta+\delta}(t)\right) \tag{32}$$

holds. Equations (30)–(32) may be solved by Fourier–Laplace transformation. For lack of space, further details of the calculation are omitted. We proceed to give the result for the long-wavelength limit of $\tilde{S}(\kappa, s)$ (equation (9)), from which the self-diffusion coefficient $D_s(c)$ is obtained via equation (10). The results read:

$$\left(\tilde{S}(\kappa \to 0, s)\right)^{-1} = s + \frac{3}{2}(1-c)^2 k^2(\kappa) + \frac{12c(1-c)^5 \beta(s) k^2(\kappa)}{1 - 2(2-5c)(1-c)^2 \beta(s)} \tag{33}$$

with

$$\beta(s) = \int\int \frac{d\sigma_1 d\sigma_2}{(2\pi)^2} \frac{e^{-i\sigma(\delta-\delta')} \sum_{\delta'} r(\delta) \cdot r(\delta')}{s + (2-c)(1-c)^2 f_1(\sigma)} \tag{34}$$

and

$$D_s(c) = \frac{3}{2}(1-c)^3 \left\{1 - \frac{8c\alpha}{2 - c - 2(2-5c)\alpha}\right\} \tag{35}$$

with

$$\alpha = \int\int \frac{d\sigma_1 d\sigma_2}{(2\pi)^2} \left(e^{-i\sigma(\delta-\delta')} \sum_{\delta'} r(\delta) \cdot r(\delta') \Big/ f_1(\sigma)\right) = (2-c)(1-c)^2 \beta(0). \tag{36}$$

It is known that α equals the average $\langle \cos\theta \rangle$ over the angle θ between the directions of two successive jumps of the tracer particle for *unconstrained* hopping in the limit of high concentration $c \to 1$. For the triangular lattice its value is $\alpha = 0.282$. The factor outside the brackets on the RHS of (35) is the short-time limit of the time-dependent self-diffusion coefficient, which for the triangular lattice is given by $\frac{3}{2}\overline{\Gamma}$, in terms of the average rate $\overline{\Gamma} = (1-c)^3$ of the jump of the tracer particle in a particular jump direction. (We set both the jump attempt frequency and the lattice constant equal to one.) The expression in the brackets on the RHS of (35) is the tracer-correlation factor f_s. The analytical result for $f_s(c)$ contained in equation (35) is compared with the Monte Carlo data for this quantity in figure 7. For lower concentrations up to about $c = 0.2$ the agreement is very good. However, for concentrations higher than $c = 0.5$ the Monte Carlo data go to zero very rapidly, whereas the approximate result tends to a non-zero limit for $c = 1$, which is given by

$$f_s(c=1) = \frac{1-2\alpha}{1+6\alpha} = 0.162. \tag{37}$$

Obviously the analytical approximation is insufficient for the higher concentrations where self-diffusion is a highly cooperative process.

6. Related models

We consider two closely related lattice-gas models, one for the same triangular lattice, but with a weaker kinetic constraint, and one for the face-centred cubic lattice. For the first of these we calculated the self-diffusion coefficient as before. For the second, three-dimensional case only a qualitative comparison with other models is made.

6.1. One-vacancy assisted hopping on the triangular lattice

For the model we investigated so far, a natural question to ask concerns the importance of the condition that *both* sites adjacent to a jump path are empty. What difference does it make if this condition is relieved and only *one* vacancy next to the path of a jumping particle is required? To answer this question we also considered the modified lattice-gas model with one-vacancy assisted hopping.

One can see immediately that this small modification of the original model changes its properties of diffusion in a fundamental way. For one-vacancy assisted hopping on the triangular lattice a vacancy can rotate around another vacancy on its nearest-neighbour sites, so that a pair of nearest-neighbour vacancies can propagate by successive rotations through an otherwise full lattice. If there is at least one pair of nearest-neighbour vacancies on a lattice, neither permanently blocked particles nor cages exist. Therefore the dynamics of the model is not cooperative in the sense described in section 2. One expects that at high concentrations ($c \to 1$) self-diffusion is governed by the interaction of one pair of nearest-neighbour vacancies with the tracer particle, as it is by the interaction between the tracer particle and a single vacancy in the case of the 'simple' lattice gas, in which only the multiple occupancy of sites is forbidden [10, 11].

These general arguments are borne out both by the Monte Carlo calculation and by an approximate analytical calculation of the tracer-correlation factor. The tracer-correlation factor is again defined by

$$f_s = D_s/\left(\tfrac{3}{2}\overline{\Gamma}\right) \tag{38}$$

where the average jump frequency $\overline{\Gamma}$ is now $\overline{\Gamma} = (1-c)(1-c^2)$, corresponding to the expression for the jump rate

$$w_{i,\delta} = (1 - n_i n_{i+\delta})\left(1 - n_{i+o(\delta)}\, n_{i+u(\delta)}\right) \tag{39}$$

instead of (26). Figure 7 also contains the Monte Carlo results for the tracer-correlation factor $f_s(c)$ for the modified model. In contrast to the results for two-vacancy assisted hopping here the correlation factor goes to a non-zero limit at $c = 1$. The analytical approximation as before is an evaluation of the long-wavelength limit of the tracer correlation function (9) in the subspace of state functions A_i (equation (22)) and B_i^{Δ} (equation (28)). The result obtained for the tracer-correlation factor reads

$$f_s(c) = 1 - \frac{2c(1+2c)^2\alpha}{(1+c)^2(2-c) - 2(1+c)(1+c-5c^2)\alpha} \tag{40}$$

which for $c = 1$ goes to the limit

$$f_s(c=1) = \frac{1-\frac{3}{2}\alpha}{1+3\alpha} = 0.312. \tag{41}$$

This result is shown by the upper dashed line in figure 7. There is qualitative agreement with the Monte Carlo data, with a maximum difference of about 50% at $c = 1$. The discrepancy at $c = 1$ is due to the fact that the approximation describes only the motion of the tracer particle and one vacancy instead of a pair of nearest-neighbour vacancies.

6.2. Four-vacancy assisted hopping on the FCC lattice

A three-dimensional analogue of our two-dimensional model is a lattice gas on the FCC lattice with four-vacancy assisted diffusion dynamics. The kinetic constraint of this model allows a particle to jump to an empty nearest-neighbour site only if the four sites adjacent to the jump path are also empty (figure 8). The distance of these sites from the jump path is $(\sqrt{3}/2)a$, if a is the nearest-neighbour distance on the FCC lattice. The kinetic constraint again has a geometric interpretation. Assume that the particles are hard spheres with diameter d in the range $(\sqrt{3}/2)a \leqslant d \leqslant a$, and that the centres of the spheres can move only on the edges of the lattice. Then a particle attempting to jump to a nearest-neighbour site cannot pass particles occupying the sites adjacent to the jump path. The particle can jump only if all four of these sites are empty. Note that the initial position i and the final position f of the jumping particle and two of the four sites adjacent to the jump path, 1 and 4 in figure 8, say, lie in a (111) plane of the FCC lattice, in which the lattice sites form a triangular lattice. Within this plane the kinetic constraint is the same as for our two-dimensional model. In three dimensions two more sites, one above and one below that plane, are required to be empty. Therefore the kinetic constraint in the three-dimensional model is more restrictive than in the two-dimensional one. Consequently, the slowing down of self-diffusion and the decrease of the self-diffusion coefficient at high particle concentrations will be even more rapid than in the two-dimensional case.

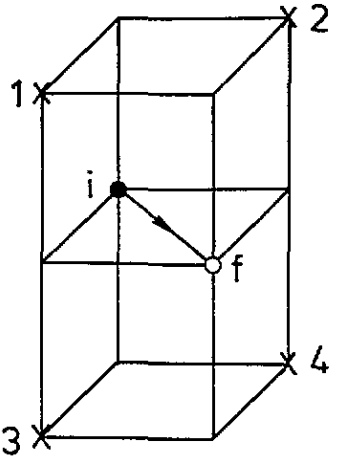

Figure 8. The kinetic constraint for a particle to jump from site i to site f in the lattice-gas model with four-vacancy assisted hopping on the FCC lattice. Sites marked 1–4 must be empty.

Like particles on a completely filled straight line in the triangular-lattice model, particles on a completely filled (111) plane in the FCC lattice model are permanently blocked. In fact, it is not necessary for the permanent blocking of particles that all sites in the plane are occupied. Several such planes oriented in different directions may form a 'cage' within which any mobile particles are trapped. In lattices of finite size a stable cage structure may exist. Whether a stable cage structure also exists in the thermodynamic limit of infinite lattice size is not clear. For the two-dimensional model we ruled out this possibility by considering a growth process in the course of which every particle on the infinite lattice performs a jump (section 4). So far we have not found a similar process for the three-dimensional model.

Since the stability of a cage structure in infinite lattices is not known, we discuss the consequences of either possibility. If the cage structure is stable, a critical concentration $c^* < 1$ must exist, above which a finite fraction of particles is permanently blocked and the self-diffusion coefficient is zero. In this case the model would be similar to a lattice gas on the simple cubic lattice with four-vacancy assisted hopping, which was studied recently by Kob and Andersen [9]. In that model it is required that a particle is always surrounded by at least three vacancies on nearest-neighbour sites. For a particle to jump at least two vacancies, in addition to the vacancy on the site of destination, must surround the site of departure, and at least two vacancies must be nearest neighbours to the site of destination. From the analysis of their Monte Carlo results for the self-diffusion coefficient the authors of the model concluded that a dynamical phase transition with critical concentration $c^* = 0.881$ exists. A similar behaviour may be expected for the constrained FCC lattice gas in the case of a stable cage structure.

If, on the other hand, the cage structure is not stable for infinite lattices, a dynamical phase transition probably does not exist. In this case, however, due to the very severe restrictions caused by the kinetic constraint at high concentrations, normal diffusion may cease to exist in the physical sense, although not in the mathematical one. This second possibility is realized by the hard-octahedron lattice gas as discussed in [8]. This is a lattice-gas model for the simple cubic lattice in which pairs of particles on nearest-neighbour sites are not allowed so that the diffusion of particles is that of hard octahedra. In [8] a proof was outlined for the instability of the cage structure in infinite lattices at all concentrations. (The maximum concentration in this model is $c_{\max} = \frac{1}{2}$.) The growth process considered in the proof is similar to one used for a bootstrap-percolation problem on the simple cubic lattice, for which the characteristic length had been shown to diverge in doubly exponential form like $\exp[a \exp(b/(c_{\max} - c))]$ with $a, b > 0$ [22]. This led to the conjecture that the self-diffusion coefficient of the hard-octahedron lattice gas for $c \to c_{\max}$ may vanish with the same functional form, namely

$$D_s(c) \propto \exp\left[-a \exp\left(b/(c_{\max} - c)\right)\right]. \tag{42}$$

If a and b are of order unity, as one expects, D_s is zero by all physical standards within an extended range of concentration. The same qualitative behaviour of $D_s(c)$ may be conjectured for the constrained FCC lattice gas model, if the same case of cage structure instability applies. We thus expect the self-diffusion coefficient for the constrained FCC lattice gas model to vanish in an extended concentration region in either case, albeit without a mathematical singularity in the latter one.

7. Size effect and characteristic length

7.1. Size dependence of the mean square displacement

As in the case of the hard-square lattice gas [7], a marked dependence of the mean square displacement on the linear dimension l of the lattice is observed for our triangular-lattice-gas model with constrained diffusion dynamics. Figure 9 shows our Monte Carlo results for concentration $c = 0.7$. For $l < 15$ the mean square displacements decrease strongly with decreasing lattice size. The curve for $l = 128$ practically coincides with that for an infinite lattice. Again as for the hard-square lattice gas the size dependence occurs already at early times, where the mean travelling distance is much shorter than the diameter of the lattice.

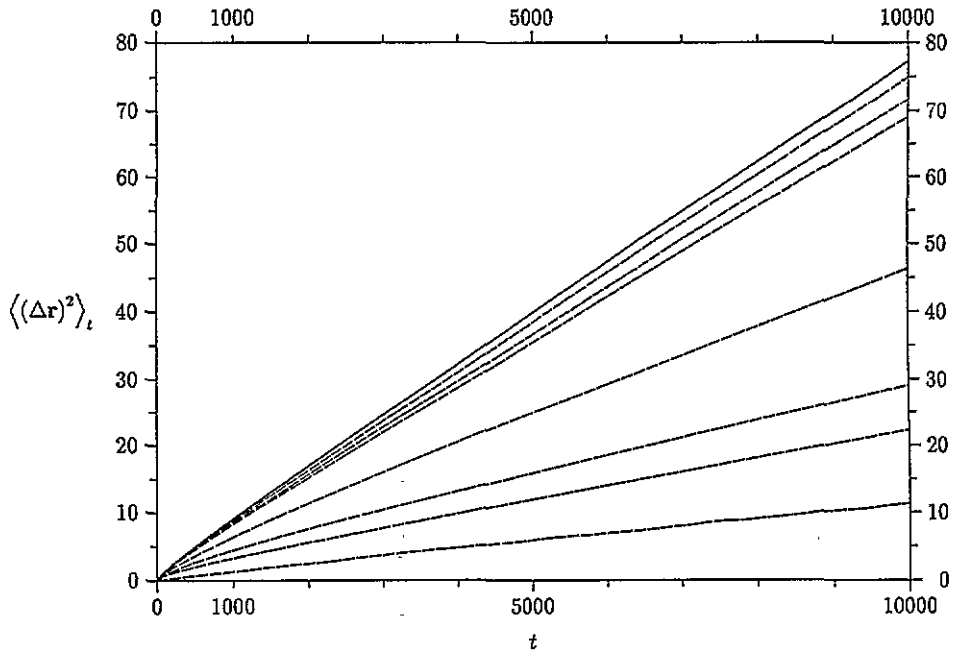

Figure 9. Size dependence of the mean square displacement against time at concentration $c = 0.7$ in lattices of size $l \times l$ with $l = 4, 6, 8, 10, 15, 20, 30$ and 128 (from the bottom).

The results shown in figure 9 are obtained for *sharp* values of the particle number density $n = N/l^2$, which are expressed as the concentration c. Normally, c is the *mean* particle number density, obtained by statistically independent filling of the lattice sites with probability c. If the lattice is populated in this latter way, the size effect is drastically different from the above for small lattice sizes. At $c = 0.7$, a size dependence in the opposite sense is observed! This surprising result is due to the fluctuations of the particle number density which become relatively large in small lattices. In a smaller lattice, configurations with a low particle density may occur, in which the mobility of the particles is strongly enhanced. The contribution of particles with fluctuation-enhanced mobility to the mean square displacement can be very large, and can outweigh the reduction of the mobility due to the smaller lattice size, which is found in configurations near the average density. The conclusion is that the size dependence of the mean square displacement typical for cooperative diffusion with kinetic constraints may be masked by the effect of particle number fluctuations in cases where the characteristic length is small. This fluctuation effect should be kept in mind when similar size effects in geometrically confined real liquids are looked for.

7.2. Characteristic length

The observed size effect indicates the existence of a characteristic length. Such a length derives from the kinetic constraint for a particle to jump, which in general requires a certain ('cooperative') rearrangement of neighbouring particles within some distance from it. To determine this distance for every particle individually is very time consuming on the computer. More efficiently, the probability distribution of such a length is obtained by counting the number of particles in a lattice of size $l \times l$ with periodic boundary

conditions which are permanently blocked. For the hard-square lattice gas this number can be determined using a cellular automaton (CA) which at every step removes all mobile particles from the lattice. (The final state reached by the CA defines a problem of 'bootstrap percolation' [20].) It is instructive to analyse the reason why this method works. On the square lattice two sublattices which are dual to one another may be distinguished. Since only jumps to nearest-neighbour sites occur in the model, a jumping particle always changes the sublattice. Through the hard-square repulsion a jump of a particle on one sublattice can be forbidden only by the presence of other particles on sites of the same sublattice. This is true for the direct blocking of a particle jump by particles on three next-nearest-neighbour sites as well as for 'blocking sequences', in which blocking particles again are blocked by other particles. Therefore, in order to find the particles which are permanently blocked on one sublattice, one needs to examine only the occupation of the sites on that same sublattice. Since a jumping particle leaves the original sublattice, a mobile particle may be removed in the process of searching for the permanently blocked particles. This justifies the method of using the CA. In addition, it follows that the permanently blocked particles are blocked already by the presence of other permanently blocked particles. The permanently blocked particles form a rigid cage structure. The other particles, which are only temporarily blocked, move around in the voids of this structure.

After this digression on the hard-square lattice gas we must address the question of whether for the triangular-lattice-gas model with two-vacancy assisted hopping the number of permanently blocked particles can also be determined by means of a CA. We first observe that our triangular-lattice-gas model does not possess the geometrical properties of the hard-square lattice gas which rigorously justify the application of a CA for that purpose. The decisive difference is that in the hard-square lattice gas a blocking sequence, in which a blocking particle may again be blocked by other particles, contains only particles on one sublattice, whereas it may contain particles on the entire lattice in our triangular-lattice-gas model. A consequence of this difference is that permanent blocking of a particle may be partly or entirely caused by particles which are *not* themselves permanently blocked. Configurations where this occurs may be obtained starting from an ordered structure with concentration $c = \frac{2}{3}$, in which the hexagonal sublattice of six-membered rings on the triangular lattice is completely filled and the dual triangular sublattice of the central sites within the rings is completely empty, and placing some particles on the triangular and some vacancies on the hexagonal sublattice. The added particles on the triangular sublattice may then be permanently blocked by the particles on the hexagonal sublattice, all or part of which are only temporarily blocked. An example of such a configuration for lattice size 6×6 (with periodic boundary conditions) is shown in figure 10. Only the two particles on the triangular sublattice, which are marked by black squares, are permanently blocked.

It is not clear how much statistical weight is carried by configurations of this sort. It may be conjectured, especially for high concentrations, that this statistical weight is low, and that in general most permanently blocked particles are blocked already by the presence of other permanently blocked particles. At any rate, this subset of permanently blocked particles, which are blocked already by the presence of other permanently blocked particles,† has properties similar to the set of permanently blocked particles in the hard-square lattice gas. It constitutes a rigid cage structure and may be obtained from the final state of a CA which at each step removes all mobile particles from the lattice. We calculated the fraction f_l of particles in this rigid cage structure using this CA for finite lattices of size $l \times l$. The results are shown in figure 11. For each value of l the curves describe the transition with increasing

† This subset is termed 'backbone' in [9].

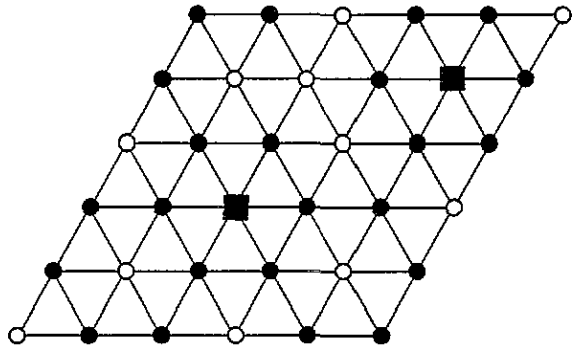

Figure 10. Example of particles (full squares) on a 6×6 lattice with periodic boundary conditions which are permanently blocked by other particles which are not themselves permanently blocked.

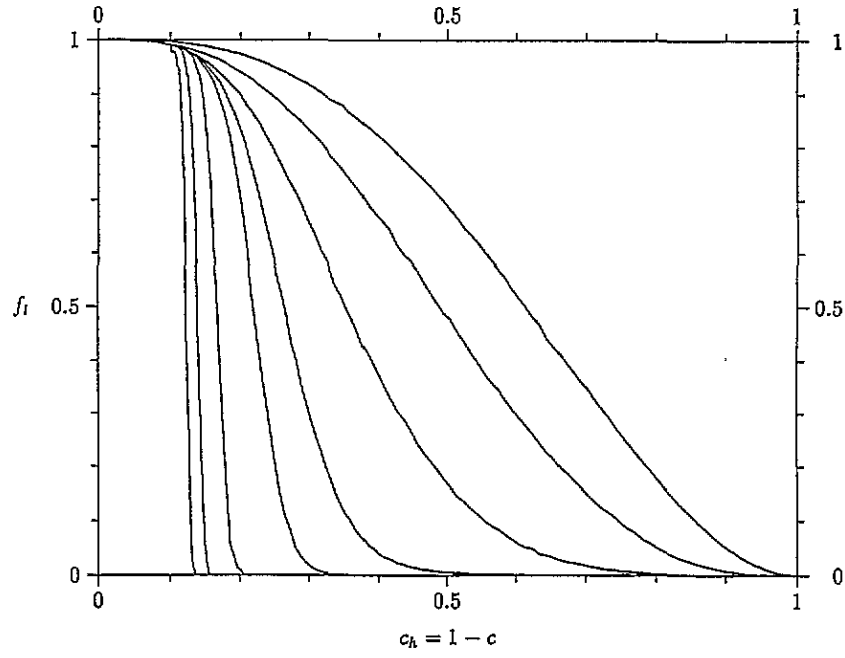

Figure 11. The fraction of particles which are permanently blocked by other permanently blocked particles as a function of particle concentration for different linear dimension l of the lattice. From right to left: $l = 2, 3, 5, 10, 20, 100, 512$ and 2048.

particle concentration from states without permanent blocking ($f_l = 0$) to states where all particles are permanently blocked ($f_l = 1$). With increasing l the transition shifts to higher particle concentration and sharpens. For $l \to \infty$ the transition shifts to $c = 1$. Similar behaviour has also been observed for the hard-square lattice gas [5], and is typical for a class of bootstrap-percolation problems [20, 23]. Quantitatively, the l-dependent transition concentration $c_p(l)$ may be defined by [19]

$$c_p(l) = -\int_0^1 c \frac{df_l}{dc} dc. \tag{43}$$

Inverting this function yields a concentration-dependent characteristic length $l_p(c)$. Results are shown in figure 12. For the highest concentrations ($0.85 \leqslant c \leqslant 0.88$) the data points follow a straight line (dashed) which is described by the formula

$$l_p(c) = 0.0128 \exp\left(\frac{1.46}{1-c}\right). \tag{44}$$

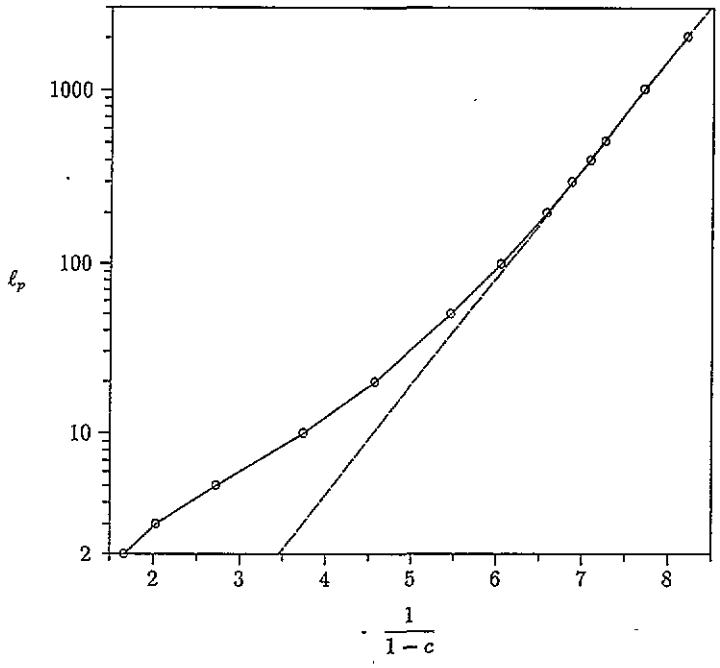

Figure 12. Characteristic length derived from fraction of permanently blocked particles (Figure 11) via equation (43) as a function of particle concentration. Dashed line is fit by equation (44).

For one concentration ($c = 0.7$) we also tested our conjecture that the fraction f_l of permanently blocked particles calculated using the CA may be a good approximation to the total fraction f_l^{total} of permanently blocked particles, which includes cases of permanent blocking by particles which are only temporarily blocked. f_l^{total} was obtained as the long-time limit ($t_{\max} = 3 \times 10^4$ MCS/particle) of the fraction of particles which in a Monte Carlo run have not moved. For sizes l ranging from 8 to 20 very good agreement between f_l^{total} and f_l was found, which supports our conjecture.

We propose that the characteristic length l_p is the relevant length for the observed size effect. This is demonstrated for the concentration $c = 0.7$. From figure 12 we deduce a value $l_p \simeq 8$, which agrees well with the range where the l dependence is strongest in figure 9. A more detailed test of our proposition is given in figure 13. Here the probability 1-f_l that a particle in a lattice of size $l \times l$ is *not* permanently blocked is plotted together with the l-dependent reduction of the mean square displacement $\langle(\Delta r)^2\rangle_t^l / \langle(\Delta r)^2\rangle_t^\infty$ at two times $t = 10^3$ and $t = 10^4$. The similarity of the two types of curve shows that the observed size effect very strongly correlates with the permanent blocking of particles in small lattices, from which the characteristic length l_p is derived.

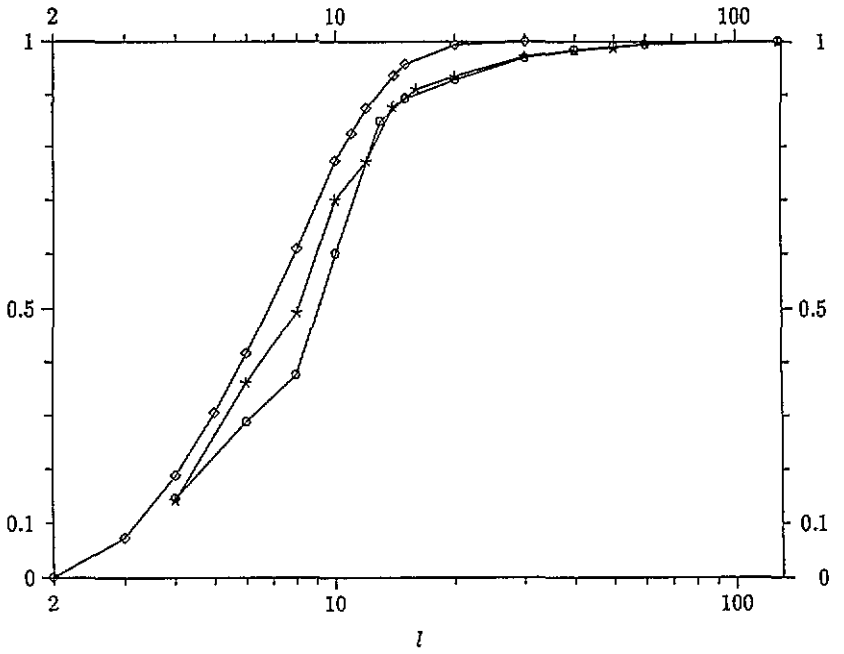

Figure 13. Comparison of the probability $1 - f_l$ that a particle is not permanently blocked by other permanently blocked particles (squares) with the ratio of reduction of the mean square displacement in a lattice of size $l \times l$ for $t = 10^3$ (stars) and $t = 10^4$ (circles) ($c = 0.7$).

8. Summary

Self-diffusion in a lattice-gas model with two-vacancy assisted hopping on the triangular lattice has been investigated, by both Monte Carlo simulation and analytical calculation. The kinetic constraint requiring two additional vacancies for a particle to jump leads to an extremely rapid decrease of self-diffusion coefficient (figure 3) and tracer-correlation factor (figure 7), and of the average relaxation rate deduced from the incoherent intermediate scattering function (figure 5), at high concentrations. In addition it causes a strong size dependence of the mean square displacement at higher concentrations (figure 9), which correlates with a characteristic length for the existence of permanently blocked particles in lattices of finite size (figure 12). All these properties are signs of pronounced cooperativity of the diffusion process at high packing density. Cooperativity of this type is absent in a variant of the model with one-vacancy assisted hopping on the same lattice. Here the tracer-correlation factor remains finite for $c \to 1$, as for the simple lattice gas without kinetic constraint.

The question of whether the model with two-vacancy assisted hopping has a dynamical phase transition at a critical concentration lower than one cannot be decided only from the Monte Carlo results for the self-diffusion coefficient. We decided against this possibility on the basis of a proof that in infinite lattices it is kinetically possible at all concentrations smaller than one to make any particle able to jump. The conjectured asymptotic concentration dependence of the self-diffusion coefficient for $c \to 1$ is of exponential form with an essential singularity at the limit $c = 1$ (equation (4)). This conjecture is supported by the concentration dependence of the characteristic length, for which the same functional form was found for lengths between 200 and 2000 (see figure 10).

An analytical calculation of the self-diffusion coefficient was carried out using a pair approximation, which is known to be very accurate in the case of the unconstrained simple lattice gas. The approximation leads to good agreement with the Monte Carlo results for the tracer-correlation factor at the lower concentrations, but fails to reproduce its very rapid decrease at the higher concentrations. We have no good analytical approximation scheme for the region of pronounced cooperativity. For the variant with one-vacancy assisted hopping, on the other hand, the same approximation qualitatively reproduces the Monte Carlo data.

We also discussed a three-dimensional variant of the model on the FCC lattice with four-vacancy assisted hopping. Here the kinetic constraint is even more restrictive than for two-vacancy assisted hopping in two dimensions. This model was compared with two other three-dimensional models with and without a dynamical phase transition: the lattice gas on the simple cubic lattice with four-vacancy assisted hopping [9] and the hard-octahedron lattice gas [8]. We argued that the very restrictive kinetic constraint of the FCC lattice-gas model will make the self-diffusion coefficient vanish in an extended concentration region in any case, either with or without a mathematical singularity at a critical concentration below one.

Acknowledgments

We acknowledge the advice of Dr K Froböse for the computer simulations. This work is part of a project supported by the Deutsche Forschungsgemeinschaft (Sonderforschungsbereich 306).

References

[1] Edwards S F and Vilgis T 1985 *Physics of Disordered Materials* ed D Adler, H Fritzsche and S R Ovshinsky (New York: Plenum) p 63; 1986 *Phys. Scrip.* T **13** 7
[2] Murch G E 1981 *Phil. Mag.* A **44** 699
[3] Chaturvedi D K 1986 *Phys. Rev.* B **34** 8080
[4] Ertel W, Froböse K and Jäckle J 1988 *J. Chem. Phys.* **88** 5027
[5] Froböse K 1989 *J. Stat. Phys.* **55** 1285
[6] Pitis R 1990 *Phys. Rev.* B **41** 7156
[7] Jäckle J, Froböse K and Knödler D 1991 *J. Stat. Phys.* **63** 249; erratum 1991 *J. Stat. Phys.* **65** 415
[8] Jäckle J 1991 *Mater. Res. Soc. Symp. Proc.* (Pittsburg, PAO Materials Research Society) vol 215 p 151
[9] Kob W and Andersen H C 1993 *Preprint*
[10] Tahir-Kheli R A and Elliott R J 1983 *Phys. Rev.* B **27** 844
[11] Tahir-Kheli R A 1983 *Phys. Rev.* B **27** 6072
[12] Kehr K 1978 *Topics in Applied Physics* ed G Alefeld and J Völkl vol 28 (Berlin: Springer) p 197
[13] Faux D A and Ross D K 1987 *J. Phys. C: Solid State Phys.* **20** 1441
[14] Adam G and Gibbs J H 1964 *J. Chem. Phys.* **43** 139
[15] Haus J W and Kehr K W 1987 *Phys. Rep.* **150** 263
[16] Taborek P, Kleiman R N and Bishop D J 1986 *Phys. Rev.* B **34** 1835
[17] Krönig A and Jäckle J 1994 *J. Phys.: Condens. Matter* **6** 7655–72
[18] Fredrickson G H and Brawer S A 1986 *J. Chem. Phys.* **84** 3351
[19] Nakanishi H and Takano H 1986 *Phys. Lett.* **115A** 117
[20] Adler J 1991 *Physica* A **171** 453
[21] Krönig A 1993 *Diploma Thesis* University of Konstanz
[22] van Enter A C D, J Adler and Duarte J A M S 1990 *J. Stat. Phys.* **60** 323
[23] Aizenman M and Lebowitz J L 1988 *J. Phys. A: Math. Gen.* **21** 3801